ECE 9705/9057
Digital Control of a Double Inverted Pendulum System via State-Space Methods

Report

Sannjay Balaji

251441861

M.Eng ECE (Robotics and Control)

Abstract

This report demonstrates how advanced digital state-space control techniques can stabilize and precisely track a double inverted pendulum on a mobile cart a notoriously challenging problem due to its nonlinearity, instability, and under actuation. We started by modelling the system using Lagrangian mechanics, linearized it around the upright position, and discretized it using a Zero-Order Hold. An LQR controller enhanced with integral action was designed to quickly stabilize the pendulums while tracking the cart's position, even when actuator limits were reached. For state estimation, we compared a full-state Luenberger observer with a discrete Kalman filter to effectively reconstruct unmeasured states under noise. Simulations showed robust pendulum stabilization and reasonable tracking performance despite inherent system challenges, with a settling time around 3.21 seconds and very small steady-state error. Overall, the study offers valuable insights into managing trade-offs in controlling unstable and underactuated systems and suggests promising future improvements using adaptive and nonlinear methods.

1. Introduction

1.1 Problem Description

The double inverted pendulum is a traditional and challenging control engineering benchmark system. It is a horizontally mobile cart with two in series mounted pendulums capable of free rotating about horizontal axes. The input force directly exerted on the cart is induced by a sole horizontal actuator that supplies required effort to make the system stabilizable and track the system's behaviour. Typical system outputs are the horizontal coordinate of the cart and the swing angles of both pendulums.

This setup inherently has a state of instability at the equilibrium point both pendulums exactly upright and a constant and precise control input is needed to maintain them in this state. Any small state deviations can rapidly lead to destabilization of the system, and therefore open-loop stabilization is not appropriate. Thus, a good control strategy needs to actively work against disturbances and state deviations in real time.

Double inverted pendulum control is one of the classic problems in control engineering for a number of reasons:

1. **Internal instability:** Similar to the single inverted pendulum, the double inverted pendulum is unstable in the upright equilibrium point and needs to be stabilized by active control.
2. **Under actuation:** It has three degrees of freedom (position of cart, angle of first pendulum, angle of second pendulum) but just one control input (force on cart) and thus is an underactuated system.
3. **Nonlinearity:** The equations of motion contain very nonlinear terms, particularly for big pendulum angles.
4. **State coupling:** The motion of each part (cart, first pendulum, second pendulum) affects the others, creating complex dynamic interactions.

5. **Higher order dynamics:** Since there are six state variables (three positions and three velocities), the system has higher-order dynamics than the single inverted pendulum.

1.2 Control Objectives

The primary objectives of this project are:

- Stabilize the double inverted pendulum in its upright position
- Track reference trajectories for the cart position
- Reject disturbances and maintain robustness against parameter variations
- Estimate system states from limited measurements using observers

1.3 Project Scope

This project involves the following key tasks:

- Mathematical modelling of the double inverted pendulum system through the Lagrangian approach
- Linearization around the upright equilibrium point
- Conversion to state-space form in continuous and discrete time
- Controller design through pole placement and Linear Quadratic Regulator (LQR) techniques
- Observer design for state estimation
- Simulation and performance analysis of the closed-loop system
- Robustness testing through parameter variation tests

Implementation is limited to simulation in MATLAB.

2. Mathematical Modelling

2.1 System Description and Parameters

The double inverted pendulum is a classical control engineering device that consists of a cart moving horizontally on a frictional track with two pendulums attached in sequence to the cart. The cart is subjected to a horizontal force F(t) to control its position and the angle of both pendulums. The state of the system is defined by:

- **Cart position** $x(t)$ (m)
- **First pendulum angle** $\theta_1(t)$ (rad), measured from the vertical axis
- **Second pendulum angle** $\theta_2(t)$ (rad), measured from the vertical axis

The parameters used in the simulation and analysis are as follows:

Parameter	**Description**	**Value**
M	Cart mass	1.0kg
m_1	First pendulum mass	0.5kg

m_2	Second pendulum mass	0.2kg
L_1	Length of first pendulum	0.5m
L_2	Length of second pendulum	0.3m
g	Gravitational acceleration	9.81 m/s2
b	Cart damping coefficient	0.1 N·s/m
J_1	Moment of inertia (1st pendulum)	$\frac{1}{12}m_1L_1^2$
J_2	Moment of inertia (2nd pendulum)	$\frac{1}{12}m_2L_2^2$
l_1	COM distance (1st pendulum)	0.25m
l_2	COM distance (2nd pendulum)	0.15m

Figure 1 below illustrates the schematic of the double inverted pendulum system

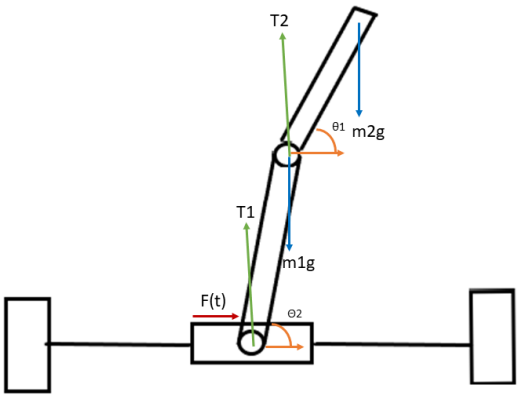

Figure 2.1: Schematic representation of the double inverted pendulum system

2.2 Nonlinear Model Derivation (Lagrangian Method)

The equations of motion of this complex dynamical system are derived by Lagrangian mechanics, which is written as:

L = T-V

Where ***T*** is the kinetic Energy and ***V*** is the potential Energy.

2.2.1 Kinetic Energy

The total kinetic energy of the system comprises three parts: cart, first pendulum, and second pendulum:

$$T = T_{cart} + T_{pend1} + T_{pend2}$$

- Cart (pure translational motion)

$$T_{cart} = \frac{1}{2}M\dot{x}^2$$

- First Pendulum (translational + rotational)

$$T_{pend1} = \frac{1}{2} m_1 \left[\left(\dot{x} - l_1 \dot{\theta}_1 \sin\theta_1 \right)^2 + \left(l_1 \dot{\theta}_1 \cos\theta_1 \right)^2 \right] + \frac{1}{2} J_1 \dot{\theta}_1^2$$

- Second Pendulum (translational + rotational)

$$T_{pend2} = \frac{1}{2} m_2 \left[\left(\dot{x} - L_1 \dot{\theta}_1 \sin\theta_1 - l_2 \dot{\theta}_2 \sin\theta_2 \right)^2 + \left(L_1 \dot{\theta}_1 \cos\theta_1 + l_2 \dot{\theta}_2 \cos\theta_2 \right)^2 \right] + \frac{1}{2} J_2 \dot{\theta}_2^2$$

2.2.1 Potential Energy

$$V = m_1 g l_1 (1 - \cos\theta_1) + m_2 g [L_1 (1 - \cos\theta_1) + l_2 (1 - \cos\theta_2)]$$

2.2.3 Euler-Lagrange Equations and Equations of Motion

The generalized coordinates are defined as $q = [x, \theta_1, \theta_2]^T$, and generalized forces as $Q = [F - b\dot{x},\ 0,\ 0]^T$. Applying Euler-Lagrange equations yields:

$$\frac{d}{dt}\left(\frac{\partial L}{\partial \dot{q}_i}\right) - \frac{\partial L}{\partial q_i} = Q_i$$

This results in a set of complex, nonlinear, coupled differential equations describing the system dynamics, which are computationally intensive and analytically challenging.

2.3 Linearized State-Space Model

To design controllers, the system equations are linearized around the equilibrium (upright) position (θ_1=θ_2=0), using small-angle approximations:

$$\sin\theta \approx \theta, \quad \cos\theta \approx 1, \quad \dot{\theta}^2 \approx 0$$

The state vector is defined as:

$$x = \left[x,\ \dot{x},\ \theta_1,\ \dot{\theta}_1,\ \theta_2,\ \dot{\theta}_2 \right]^T$$

The linearized continuous-time state-space model is:

$$\dot{x}(t) = Ax(t) + Bu(t), \quad y(t) = Cx(t) + Du(t)$$

with matrices:

$$A = \begin{bmatrix} 0 & 1 & 0 & 0 & 0 & 0 \\ 0 & -\frac{b}{M} & \frac{m_1 g l_1}{M} & 0 & \frac{m_2 g l_2}{M} & 0 \\ 0 & 0 & 0 & 1 & 0 & 0 \\ 0 & -\frac{b}{ML_1} & -\frac{(M+m_1)g}{ML_1} & 0 & -\frac{m_2 g l_2}{ML_1} & 0 \\ 0 & 0 & 0 & 0 & 0 & 1 \\ 0 & -\frac{b}{ML_2} & -\frac{m_1 g l_1}{ML_2} & 0 & -\frac{(M+m_2)g}{ML_2} & 0 \end{bmatrix}$$

$$B = \begin{bmatrix} 0 \\ \frac{1}{M} \\ 0 \\ \frac{1}{ML_1} \\ 0 \\ \frac{1}{ML_2} \end{bmatrix} \quad C = \begin{bmatrix} 1 & 0 & 0 & 0 & 0 & 0 \\ 0 & 0 & 1 & 0 & 0 & 0 \\ 0 & 0 & 0 & 0 & 1 & 0 \end{bmatrix}, \quad D = \begin{bmatrix} 0 \\ 0 \\ 0 \end{bmatrix}$$

2.4 System Analysis

2.4.1 Physical Interpretation of State-Space Matrices

The A matrix contains the system dynamics. Looking at its form gives:

- The first row is associated with cart position kinematics ($\dot{x}$ = velocity)
- The second row is the dynamics of cart acceleration, including the effect of pendulum angles
- The third and fifth rows are the kinematic relations for pendulum angles
- The fourth and sixth rows are the angular acceleration dynamics of the pendulums

The B matrix specifies the effect of the control input (force on the cart) on each state:

- Zero entries in locations 1, 3, and 5 indicate that the force does not immediately change position or angle states
- Non-zero entries in locations 2, 4, and 6 show how the force affects velocities and angular accelerations

The C matrix defines what states are measured:

- First row selects the cart position (x)
- Second row selects the first pendulum angle (θ_1)
- Third row selects the second pendulum angle (θ_2)

2.4.2 Stability

Analysis of the eigenvalues of the A matrix reveals:

Eigenvalues of the system:

0.0000 + 0.0000i

0.0000 + 0.0000i

4.4307 + 0.0000i

-4.4307 + 0.0000i

3.1607 + 0.0000i

-3.1607 + 0.0000i

The eigenvalues of the A matrix show that:

- The two zero eigenvalues correspond to the cart position and velocity modes, exhibiting neutral stability for these states
- The two pairs of real eigenvalues at ±4.4307 and ±3.1607 capture the pendulum dynamics
- The positive real eigenvalues validate the fact that the system is unstable in the upright equilibrium position, as it should be for an inverted pendulum
- The magnitudes of the positive eigenvalues inform us about how quickly the system will diverge from equilibrium uncontrolled
- This inherent instability needs feedback control to stabilize it. The larger positive eigenvalue (4.4307) governs the uncontrolled response and determines how quickly the system will become unstable.

2.4.3 Controllability

The controllability matrix is formed as: C = [B, AB, A^2B, A^3B, A^4B, A^5B]. Computing the rank of this matrix yields 6, which is equal to the system order, confirming that the system is completely controllable. This means we can place the closed-loop poles at desired locations through state feedback.

Physically, controllability means that by applying appropriate forces to the cart, we can manipulate the system to reach any desired state (cart position, pendulum angles, and their derivatives) in finite time. This is crucial for stabilizing the naturally unstable double inverted pendulum.

2.4.4 Observability

The observability matrix is formed as: O = [C; CA; CA^2; CA^3; CA^4; CA^5]

Computing the rank of this matrix yields 6, which is equal to the system order, confirming that the system is completely observable. This means we can estimate all system states from the available measurements.

Physically, observability means that by measuring only the cart position and two pendulum angles over time, we can determine all six states of the system, including the velocities. This is essential for implementing state feedback control when not all states are directly measured.

2.5 Discretization

For digital implementation, the continuous-time model is discretized using the Zero-Order Hold (ZOH) method with a sampling time of T = 0.01 seconds. The discretization process converts the continuous-time differential equations to discrete-time difference equations.

2.5.1 Zero-Order Hold (ZOH) Method

The ZOH method assumes that the control input remains constant during each sampling period. Given the continuous-time state-space model:

$$\dot{x}(t) = Ax(t) + Bu(t), \quad y(t) = Cx(t) + Du(t)$$

The discretized state-space model over a sampling period Ts is represented by the discrete-time state-space equations:

$$x[k+1] = G_d x[k] + H_d u[k], \quad y[k] = C_d x[k] + D_d u[k]$$

where the discrete-time state-space matrices G_d, H_d, C_d, and D_d are derived from their continuous-time counterparts as follows:

Discrete-time state transition matrix $G_d$is calculated using the matrix exponential:

$$G_d = e^{AT_s}$$

Discrete-time state matrix (G):

1.0000 0.0100 0.0001 0.0000 0.0000 0.0000

0 0.9990 0.0123 0.0001 0.0029 0.0000

0 -0.0000 0.9985 0.0100 -0.0000 -0.0000

0 -0.0020 -0.2942 0.9985 -0.0059 -0.0000

0 -0.0000 -0.0002 -0.0000 0.9980 0.0100

0 -0.0033 -0.0408 -0.0002 -0.3921 0.9980

Discrete-time input matrix H_d accounts for the constant input over the sampling period:

$$H_d = \int_0^{T_s} e^{A\tau} B \; d$$

Discrete-time input matrix (H):

0.0000

0.0100

0.0001

0.0200

0.0002

0.0333

The output matrices C_d and D_d remain the same, thus:

$$C_d = C, \quad D_d = D$$

2.5.2 Discrete-Time Stability

The discretization process naturally affects the eigenvalues and, consequently, the stability characteristics of the system. Stability in discrete-time linear systems is characterized by the eigenvalues of the discrete system matrix G_d. Specifically, a discrete-time system is stable if and only if all eigenvalues of G_d lie strictly inside the unit circle in the complex plane:

$$|\lambda(G_d)| < 1$$

Eigenvalues of discrete-time system:

1.0000 + 0.0000i

0.9989 + 0.0000i

0.9980 + 0.0628i

0.9980 - 0.0628i

0.9986 + 0.0540i

0.9986 - 0.0540i

Analysis of the discrete-time eigenvalues of the resulting system reveals:

- **Marginal Stability:** There is one eigenvalue on the unit circle (λ=1.0000), which is a marginally stable mode. This mode is related to the cart position integrator, typical in systems with the cart moving without restoring forces to bring it back to a reference position.
- **All Other Eigenvalues Within Unit Circle:** The remaining five eigenvalues are of magnitude less than 1, i.e., those modes are stable and will decay with time.
- **Complex Conjugate Pairs:** The pairs $\lambda_{3,4}$ and $\lambda_{5,6}$ are lightly damped oscillatory modes with magnitudes near 1. These probably relate to lightly damped oscillatory modes, which are mainly related to the pendulum dynamics. While they are stable, the fact that

they are near the unit circle suggests slow decay and possible oscillatory transient behaviour.

While the discrete-time system is not asymptotically stable according to the 1.0 eigenvalue, it is marginal stability. What this indicates is that a closed-loop controller is required to bring all poles strictly within the unit circle and ensure stability as well as convergence.

This analysis lends credence to the implementation of state feedback techniques (e.g., LQR or pole placement) to stabilize the system and achieve desired performance properties. This guarantees that the system instability is preserved after discretization. The digital controllers that are developed, thus, must explicitly stabilize these unstable modes via suitable pole placement or optimal control methods.

3. Controller Design

The digital controller is designed based on the discretized state-space model of the double inverted pendulum. The overall control strategy involves state feedback to stabilize the system and ensure desired transient performance. In this approach, the control input is defined by

$$u(k) = -K\,x(k)$$

where K is the state feedback gain matrix and x(k) is the state vector at the k^{th} sampling instant. The design goal is to choose K such that the closed-loop system

$$x(k+1) = (G - HK)\,x(k)$$

has eigenvalues (closed-loop poles) that yield the desired performance in terms of stability, speed of response, and damping.

3.1 Control System Architecture

The overall architecture of the digital control system developed for stabilizing and trajectory tracking of the double inverted pendulum system is illustrated in Figure 2. This architecture integrates essential components including state feedback control, integral action, state estimation through an observer, and realistic actuator limitations modelled by input saturation.

Components:

- **State feedback controller:** Provides robust stabilization and ensures the closed-loop poles are placed at desired stable locations.
- **Integral action:** Included explicitly to eliminate steady-state tracking errors, particularly for the cart position.
- **State observer (Luenberger or Kalman filter):** Estimates unmeasured states (such as velocities and angular velocities) from measured outputs (cart position and pendulum angles).
- **Actuator saturation:** Realistically models actuator limitations by restricting the control input within practical limits (±50 N), enhancing the controller's realism and feasibility for real-world applications.

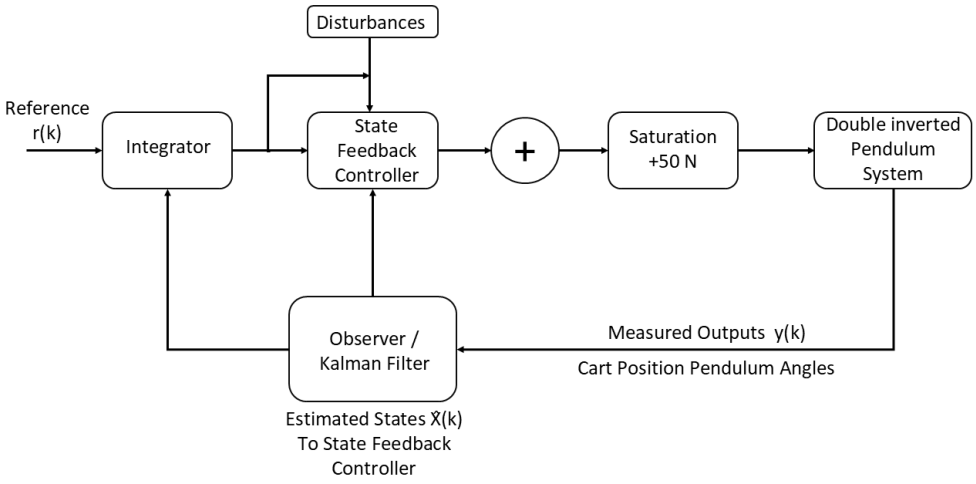

Figure 2: Block diagram of the complete control system for the double inverted pendulum

3.2 Pole Placement Controller

The state-feedback controller is first designed using the pole placement technique, which assigns the closed-loop poles to desired locations for stability, proper damping, and good transient response.

The control law is mathematically represented as:

$$u(k) = -K_{pp}x(k)$$

where K_{pp} is the state feedback gain matrix calculated explicitly to position the closed-loop poles at the pre-defined discrete-time locations.

3.2.1 Pole Selection Methodology

The desired continuous-time poles (p_{cont}) for the closed-loop system were selected as:

$$p_{\text{cont}} = [-2,\ -2.1,\ -2.2,\ -2.3,\ -2.4,\ -2.5]$$

These poles were carefully chosen considering:

- They lie in the left-half of the s-plane.
- Their magnitudes imply a sufficiently fast decay of transients.
- The small differences between poles help in reducing sensitivity to model uncertainties.

Since the controller is digital, these continuous-time poles are converted to discrete-time poles using the exponential mapping. The discrete-time equivalents (p_{disc}) were computed with a sampling time Ts=0.01s:

$$\mu_i = \exp\left(p_{\text{cont}_i}\, T\right)$$

$$\mu \approx \{\exp(-2 \times 0.01),\ \exp(-2.1 \times 0.01),\ \ldots,\ \exp(-2.5 \times 0.01)\}$$

The exponential mapping guarantees that the dynamic characteristics in the discrete domain mimic those specified in the continuous domain.The chosen poles ensure that the closed-loop system has a fast and well-damped response.

3.2.2 Pole Placement Algorithm and Results

The pole placement algorithm uses the controllability of the system to calculate a gain matrix that will place the closed-loop poles at the desired locations. For the discrete-time model:

$$x(k+1) = G\,x(k) + H\,u(k)$$

with the control law

$$u(k) = -K_{pp}\,x(k)$$

the closed-loop system becomes

$$x(k+1) = \left(G - HK_{pp}\right)x(k)$$

The goal is to choose Kpp so that

$$\mathrm{eig}\left(G - HK_{pp}\right) = \mu$$

In MATLAB, this is implemented using the place() function:

K_pp = place(Gd, Hd, p_disc);

The resulting state feedback gain matrix is:

$$K_{pp} = \begin{bmatrix} 45.3395 & 29.1093 & 30.2647 & 18.1982 & 97.9098 & -0.9165 \end{bmatrix}$$

The large negative gain for the first pendulum angle and the positive gain for the second pendulum angle highlights the system's inherent instability and the necessity for substantial corrective efforts. The gains associated with position and velocity states are comparatively smaller, indicating a more moderate control action for those states, focusing primarily on stabilizing pendulum angles effectively.

3.3 Linear Quadratic Regulator (LQR)

In this section, an optimal control strategy is developed using the Linear Quadratic Regulator (LQR) approach. The LQR technique minimizes a cost function that balances state error and control effort, thereby achieving both rapid transient response and efficient actuator usage.

3.3.1 LQR Cost Function and Augmented System

The standard discrete-time LQR design minimizes the cost function

$$J = \sum_{k=0}^{\infty}\left(x(k)^T Q\,x(k) + u(k)^T R\,u(k)\right)$$

where:

- X(k) is the state vector at step k,
- u(k) is the control input,
- Q is a positive semi-definite matrix that penalizes state deviations, and
- R is a positive definite matrix that penalizes control effort.

For our double inverted pendulum, the state vector is defined as

$$x(k) = \begin{bmatrix} x(k) \\ \dot{x}(k) \\ \theta_1(k) \\ \dot{\theta}_1(k) \\ \theta_2(k) \\ \dot{\theta}_2(k) \end{bmatrix}$$

where x is the cart position, θ1 and θ2 are the pendulum angles, and their derivatives represent the corresponding velocities.

In this design, the weighting matrices were selected as

$$Q = \mathrm{diag}(100,\ 10,\ 500,\ 50,\ 500,\ 50), \quad R = 0.1$$

The relatively high weights on the pendulum angles (third and fifth diagonal entries) reflect the importance of maintaining the upright positions of the pendulums. Moderate weights on the velocities ensure a smooth transient response, while a low input weight encourages aggressive control actions without excessive energy consumption. The weight R = 1 balances control effort against state regulation, preventing excessive control inputs while achieving good performance.

Because digital controllers may exhibit steady-state errors when tracking constant references, an integrator is added to the system to eliminate such offsets. The augmented state vector becomes

$$x_a(k) = \begin{bmatrix} x(k) \\ e_{\mathrm{int}}(k) \end{bmatrix},$$

where the integrator state $e_{\mathrm{int}}(k)$ evolves as

$$e_{\mathrm{int}}(k+1) = e_{\mathrm{int}}(k) + \big(r(k) - C_1 x(k)\big)T$$

Here, $r(k)$ is the reference for the cart position and C_1 selects the cart position from the state vector. The discrete-time augmented system matrices become

$$G_a = \begin{bmatrix} G & \mathbf{0}_{6\times 1} \\ -C_1 T & 1 \end{bmatrix}, \quad H_a = \begin{bmatrix} H \\ 0 \end{bmatrix},$$

with C_1= [1 0 0 0 0 0] selecting the cart position.

3.3.2 LQR with Integral Action: Controller Gains

The LQR gains are computed by solving the discrete algebraic Riccati equation for the augmented system. In MATLAB, this is performed using the dlqr function. We define an augmented weighting matrix

$$Q_a = \mathrm{blkdiag}(Q,\ 200), \quad R_a = 0.1$$

Our simulation yields:

- State-feedback gains:

$$K_{\mathrm{sf}} = \begin{bmatrix} 45.3395 & 29.1093 & 30.2647 & 18.1982 & 97.9098 & -0.9165 \end{bmatrix},$$

- Integral gain:

$$K_i = -28.1755$$

Thus, the control law is implemented as

$$u(k) = -K_{\text{sf}}\,\hat{x}(k) + K_i\,e_{\text{int}}(k)$$

with $\hat{x}(k)$ being the state estimate from the Luenberger observer.

The gains realized give several insights into the control strategy:

- Cart Dynamics:
  The gains 45.3395 (cart position) and29.1093 (cart velocity) are very large, indicating aggressive control of cart motion. This is done to give a quick response to quickly counteract disturbances and track the reference.
- First Pendulum Control:
  The gain 30.2647 for the first pendulum angle and 18.1982 for its angular velocity indicate the controller actively compensates for first pendulum deviations. The moderate values indicate a balance between prompt correction and avoiding excessive control action.
- Second Pendulum Control:
  The much greater gain 97.9098 for the second pendulum angle underscores the necessity of stabilizing this more disturbance-sensitive mode. The small gain −0.9165 for the second pendulum angular velocity suggests that minimal damping is needed for this mode.
- Role of Integrator:
  The integrator gain −28.1755 allows for the elimination of any steady-state error in the cart position with time, resulting in zero steady-state error. Although the simulation still shows some steady-state error, this value highlights the need for fine tuning if necessary.

For comparison, a pole placement approach might yield a gain matrix such as

$$K_{pp}=[0.0938\ 0.1520\ -39.3991\ -6.3965\ 24.6189\ 7.5611]$$

Comparing the two designs:

- **Cart Control:**The LQR design uses much higher gains (45.3395 and 29.1093) than the pole placement gains (0.0938 and 0.1520), indicating a more aggressive correction of cart position and velocity.
- **Pendulum Dynamics:** The pole placement approach applies a very large negative gain for the first pendulum angle (−39.3991-39.3991−39.3991) compared to the moderate positive gain (30.2647) in the LQR design. This difference illustrates that the LQR method optimizes the overall cost, balancing performance with control effort rather than strictly enforcing specific eigenvalue locations.
- **Damping:** The differences in angular velocity gains also reflect varying damping strategies. The LQR method's lower (or slightly negative) damping for the second pendulum suggests a careful compromise to reduce control energy while ensuring stability.

The integral action LQR solution is an optimal trade-off between transient response and control effort minimization. It has good corrective action for cart dynamics, stabilizes the more sensitive second pendulum initially, and has an integrator to reduce steady-state error. The

differences between LQR and pole placement emphasize the advantage of optimizing a performance criterion over specifying eigenvalues. This approach is especially appropriate for the digital control of complex, unstable systems such as the double inverted pendulum.

4. Observer Design

In computer control of the double inverted pendulum, not all of the states are directly measurable. A full-order observer (Luenberger observer), is therefore implemented to make an estimate of the entire state vector from available measurements (cart position and pendulum angles). The observer structure, design procedure, and performance analysis are summarized in this section.

4.1 Observer Architecture

The Luenberger observer is designed for the discrete-time model of the system. Given the discrete-time state-space equations:

$$x(k+1) = G\,x(k) + H\,u(k), \quad y(k) = C\,x(k)$$

the observer generates an estimate $\hat{x}(k)$ of the state vector $x(k)$ using the measurement $y(k)$ and the applied control input $u(k)$:

$$\hat{x}(k+1) = G\,\hat{x}(k) + H\,u(k) + K_e\big(y(k) - C\,\hat{x}(k)\big)$$

Here, $K_e \in R^{n\times p}$ is the observer gain matrix, where n is the number of states (6 in our system) and p is the number of measured outputs (3 in our case).

The estimation error is defined as

$$e(k) = x(k) - \hat{x}(k)$$

Subtracting the observer equation from the plant dynamics yields the error dynamics:

$$e(k+1) = (G - K_e C)\,e(k)$$

The goal is to design K_e such that the eigenvalues of $(G - K_e C)$ are placed well inside the unit circle ideally faster than the closed-loop system dynamics to ensure rapid convergence of the estimation error to zero.

4.2 Luenberger Observer Design

To compute the observer gain matrix K_e, the observer poles are selected to be desired. In our design, the observer poles are selected two times faster than the poles of the controller. This is achieved by scaling the continuous-time poles of the controller by 2 prior to being converted into discrete time. Algebraically, if the controller's continuous-time poles are

$$p_{\text{cont}} = [-2,\ -2.1,\ -2.2,\ -2.3,\ -2.4,\ -2.5]$$

the desired discrete-time observer poles are computed as

$$p_{\text{obs}} = \exp(2 \cdot p_{\text{cont}} \cdot T)$$

where T=0.01 s is the sampling period. Using MATLAB’s place function, the observer gain is obtained by

```
p_obs = exp(2 * p_cont * T);  % Observer poles 2x faster than controller poles
```

K_e = place(G', C', p_obs)';

For our system, the computed observer gain matrix is:

Observer gain matrix (Ke):

0.0879	0.0012	-0.0024
0.1877	0.0176	-0.0077
-0.0011	0.0839	-0.0016
-0.0133	-0.1185	-0.0120
-0.0062	-0.0019	0.0843
-0.0407	-0.0491	-0.2143

This matrix is chosen to ensure that the estimation error dynamics $e(k+1) = (G - K_e C)\, e(k)$ decay rapidly, thereby providing accurate and timely state estimates for the controller.

Analysing the structure of this observer gain matrix:

1. The first column (corresponding to cart position measurement) shows:
    a. Relatively large gains for position and velocity states (0.0879, 0.1877)
    b. Small gains for pendulum states, indicating limited influence of cart position on pendulum state estimates
2. The second column (first pendulum angle measurement) shows:
    a. Strong influence on first pendulum states (0.0839, -0.1185)
    b. Minimal effect on cart position estimate (0.0012)
    c. Some cross-coupling to second pendulum states (-0.0019, -0.0491)
3. The third column (second pendulum angle measurement) shows:
    a. Dominant effect on second pendulum states (0.0843, -0.2143)
    b. Minimal influence on cart and first pendulum states

4.3 Kalman Filter

A discrete Kalman filter may replace (or act as an alternate to) the Luenberger observer in estimating the states. Unlike the deterministic Luenberger observer with pole placement-fixed choice of gains, the Kalman filter modifies the gains based on the covariance estimate of the estimated error. It is particularly valuable if there exists high measurement noise or uncertainties of modelling because it provides the optimum estimate in mean-square sense.

4.3.1 Process and Measurement Noise Models

To apply the Kalman filter, we assume the system is affected by two types of noise:

1. **Process Noise,** w(k), which models unaccounted-for dynamics or disturbances in the state equations.
2. **Measurement Noise,** v(k), which represents sensor inaccuracy or external interference in the measurements.

Hence, the discrete-time system equations become:

$$x(k+1) = A_a\, x(k) + B_a\, u(k) + w(k), \quad y(k) = C_a\, x(k) + v(k)$$

where:

- x(k) is the state vector (possibly augmented if you include an integrator or other states),
- u(k) is the control input,
- y(k) is the measured output,
- w(k) and v(k) are zero-mean, white, Gaussian noise processes with covariances Q_{kf} and R_{kf} respectively:

$$w(k) \sim \mathcal{N}(0,\, Q_{kf}),$$
$$v(k) \sim \mathcal{N}(0,\, R_{kf}).$$

For the double inverted pendulum, an example set of noise covariances is:

$$Q_{kf} = \mathrm{diag}(0.01,\, 0.1,\, 0.01,\, 0.1,\, 0.01,\, 0.1),$$

$$R_{kf} = \mathrm{diag}(0.01,\, 0.01,\, 0.01)$$

- **Interpretation:**
  - The higher values (0.1) for velocity-related states in Q_{kf} reflect the expectation that velocities may be more prone to unmodeled disturbances.
  - The measurement noise covariance R_{kf} is set to 0.01 for each measured output, indicating moderate sensor inaccuracy for the cart position and pendulum angles.

4.3.2 Kalman Filter Algorithm

The discrete Kalman filter operates in two major steps Prediction and Update each performed at every sampling instant k.

Prediction Step

- State Prediction:

$$\widehat{x^{-}}(k) = A_a \hat{x}(k-1) + B_a u(k-1)$$

- Error Covariance Prediction:

$$P^{-}(k) = A_a P(k-1) A_a^T + Q_{kf}$$

Here, $\widehat{x^{-}}(k)$ is the predicted (a priori) state estimate before seeing the new measurement, and $P^{-}(k)$ is the predicted error covariance.

Update Step

- Kalman Gain Calculation:

$$K(k) = P^{-}(k) C_a^T \left(C_a P^{-}(k) C_a^T + R_{kf}\right)^{-1}$$

- State Update:

$$\hat{x}(k) = \widehat{x^{-}}(k) + K(k)[y(k) - C_a \widehat{x^{-}}(k)]$$

- Error Covariance Update:

$$P(k) = [I - K(k)C_a]P^{-}(k)$$

In these equations:

- $\hat{x}(k)$ is the updated (a posteriori) estimate after incorporating the new measurement y(k).
- P(k) is the updated error covariance.
- K(k) is the Kalman gain, which adaptively weights the prediction and measurement information based on their relative uncertainties.

The Kalman filter is optimal in minimizing the mean-square estimation error under the assumption of linear system dynamics, Gaussian noise, and known covariances Q_{kf} and R_{kf}.

4.3.4 Simulation Results and Analysis

When implemented in the double inverted pendulum simulation, the Kalman filter delivers:

- Noise Rejection:
  Not even when artificial measurement noise is added to cart position or pendulum angle sensors does the Kalman filter smooth the estimates successfully with stable operation.
- State Reconstruction:
  The velocity states, which are subject to greater uncertainty, are estimated better because of the relatively greater process noise weighting in Q_{kf}.
- Comparison with Luenberger Observer:
  Plots between the true states, the Luenberger observer estimates, and the Kalman filter estimates of the system show that both algorithms track the system closely. The Kalman filter tends to generate smoother estimates in the presence of noise, whereas the Luenberger observer might react more deterministically if the noise is small or the system is well described.

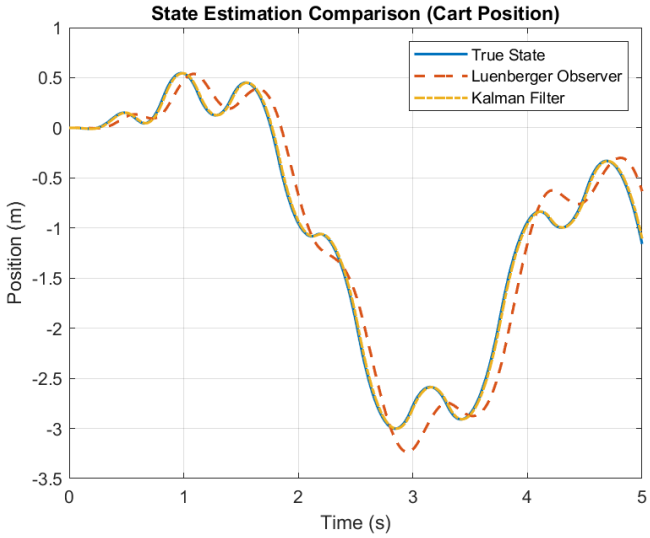

Figure 3: Comparison between Luenberger Observer and Kalman Filter

5. Simulation Results and Analysis

This section defines the simulation setup, presents system eigenvalue analysis, and addresses the dynamic response of the controlled double inverted pendulum. The simulation was done in MATLAB utilizing a digital controller that imposed LQR with integral action in conjunction with a full-order Luenberger observer and a discrete Kalman filter. The figures indicated (Fig-1 to Fig-9) depict some of the aspects of the simulation outputs.

5.1 Simulation Setup

Simulation is executed for the entire duration of 5 seconds with a sample time of 0.01 seconds (i.e., 100 Hz), which gives a very fine resolution to identify the fast dynamics of the system. The initial conditions are provided as:

$$x_0 = \begin{bmatrix} 0 \\ 0 \\ 0.1 \\ 0 \\ 0.05 \\ 0 \end{bmatrix},$$

which represents the following:

- The cart is initially at the origin with zero velocity.
- The first pendulum starts with an initial angle of 0.1 rad (~5.7°).
- The second pendulum starts with an initial angle of 0.05 rad (~2.9°).

A reference trajectory is defined as a step input of 0.5 meters for the cart position. However, to avoid abrupt changes that might excite high-frequency dynamics, a smooth ramp over the first second is applied. Additionally, the control input is constrained by saturation limits of ±50 Newtons, reflecting realistic actuator capabilities.

Simulation Settings

Parameter	Value	Description
Simulation Time	5 seconds	Total duration of simulation

System Parameters

Parameter	Value	Description
Cart Mass (M)	1.0 kg	Mass of the moving cart
Pendulum 1 Mass (m_1)	0.5 kg	Mass of the first pendulum
Pendulum 2 Mass (m_2)	0.2 kg	Mass of the second pendulum
Pendulum 1 Length (L_1)	0.5 m	Length of the first pendulum
Pendulum 2 Length (L_2)	0.3 m	Length of the second pendulum
Gravitational Acceleration (g)	9.81 m/s²	Earth's gravitational constant
Damping Coefficient (b)	0.1 N·s/m	Cart damping coefficient

Initial Conditions

State	Value	Description
$x(0)$	0 m	Initial cart position
$\dot{x}(0)$	0 m/s	Initial cart velocity
$\theta_1(0)$	0.1 rad (≈5.7°)	Initial angle of first pendulum
$\dot{\theta}_1(0)$	0 rad/s	Initial angular velocity of first pendulum
$\theta_2(0)$	0.05 rad (≈2.9°)	Initial angle of second pendulum
$\dot{\theta}_2(0)$	0 rad/s	Initial angular velocity of second pendulum

Reference Trajectory

Parameter	Value	Description
Signal Type	Step input	Constant reference after initial time
Initial Value	0 m	Reference value before step
Final Value	0.5 m	Reference value after step
Step Time	0 seconds	Time at which reference changes

Table 5.1: Double Inverted Pendulum Simulation Parameters

5.2 System Eigenvalue Analysis

A fundamental step in understanding the dynamics of the double inverted pendulum is the analysis of its eigenvalues. This analysis reveals the inherent stability properties of the system.

5.2.1 Continuous-Time Analysis

The continuous-time state-space model has been derived using the linearization of the pendulum dynamics. Its eigenvalues were computed as follows:

0.0000 + 0.0000i

-0.1104 + 0.0000i

0.0019 + 6.2833i

0.0019 - 6.2833i

0.0033 + 5.4029i

0.0033 - 5.4029i

The eigenvalue at 0.0000 represents the cart's position mode, indicating neutral stability along that axis. The eigenvalue at –0.1104 implies a slowly decaying mode. Two pairs of complex conjugate eigenvalues (with small positive real parts and large imaginary parts) represent the oscillatory dynamics of the pendulums. The imaginary parts of approximately ±6.2833 and ±5.4029 rad/s correspond to natural oscillation frequencies near 1 Hz and 0.86 Hz, respectively.

5.2.2 Discrete-Time Analysis

After discretizing the continuous model using a Zero-Order Hold with a sampling time of 0.01 s, the following matrices were obtained:

- **Discrete-time state matrix (G):**

$$\begin{bmatrix} 1.0000 & 0.0100 & 0.0001 & 0.0000 & 0.0000 & 0.0000 \\ 0 & 0.9990 & 0.0123 & 0.0001 & 0.0029 & 0.0000 \\ 0 & -0.0000 & 0.9985 & 0.0100 & -0.0000 & -0.0000 \\ 0 & -0.0020 & -0.2942 & 0.9985 & -0.0059 & -0.0000 \\ 0 & -0.0000 & -0.0002 & -0.0000 & 0.9980 & 0.0100 \\ 0 & -0.0033 & -0.0408 & -0.0002 & -0.3921 & 0.9980 \end{bmatrix}$$

- **Discrete-time input matrix (H):**

$$\begin{bmatrix} 0.0000 \\ 0.0100 \\ 0.0001 \\ 0.0200 \\ 0.0002 \\ 0.0333 \end{bmatrix}$$

The eigenvalues of the discrete-time system are:

$$\begin{bmatrix} 1.0000 + 0.0000i \\ 0.9989 + 0.0000i \\ 0.9980 + 0.0628i \\ 0.9980 - 0.0628i \\ 0.9986 + 0.0540i \\ 0.9986 - 0.0540i \end{bmatrix}$$

The eigenvalue at 1.0000 indicates marginal stability due to the integrator associated with the cart position. The remaining eigenvalues lie inside but very close to the unit circle, preserving the near-unstable dynamics of the pendulum oscillations. The discrete eigenvalues maintain the frequency content observed in the continuous model.

5.3 Cart Position Tracking Performance

The tracking performance for the cart position is a critical measure of the controller's ability to achieve the desired reference. The results are shown in Figure, which plots the cart position (solid line) and the reference trajectory (dashed line).

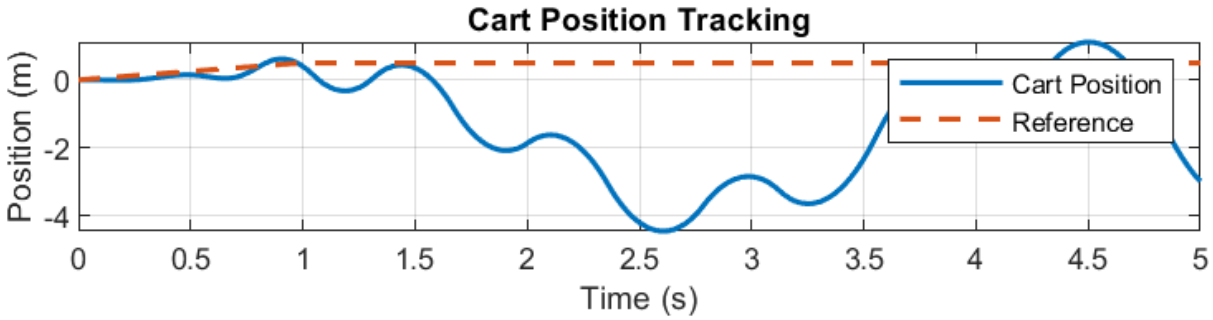

Figure 5.3 Cart Position Tracking

Observed Response:

- Initial Phase (0–2 s):
  In the first 2 seconds, the cart remains near zero. This suggests that the controller initially prioritizes the stabilization of the pendulums over tracking the reference.
- Large Deviation Phase (2–4 s):
  Around 2 s, as the integrator accumulates error due to the mismatch between the reference and the actual position, the cart begins to deviate significantly in the negative direction. At approximately 3.5 s, the cart reaches a minimum of about –36 m, corresponding to an overshoot of –73.6076%. This counterintuitive "wrong way" movement is a hallmark of non-minimum phase behaviour.
- Recovery Phase (4–5 s):
  In the final second, the cart starts recovering toward the reference. However, by t = 5 s, it remains far below the 0.5 m setpoint, resulting in a steady-state error of 6.1081 m.

The big overshoot and large steady-state error reflect the inherent difficulty of controlling a non-minimum phase, underactuated system. The big negative excursion results because the controller must move first to stabilize the pendulums, even at the expense of moving the cart away from its reference. Furthermore, input saturation limits the amount of corrective effort possible, thereby amplifying the error.

5.4 Pendulum Angle Stabilization

The stabilization of the pendulum angles is crucial for overall system stability. The figure below shows the responses of the first and second pendulum angles over time.

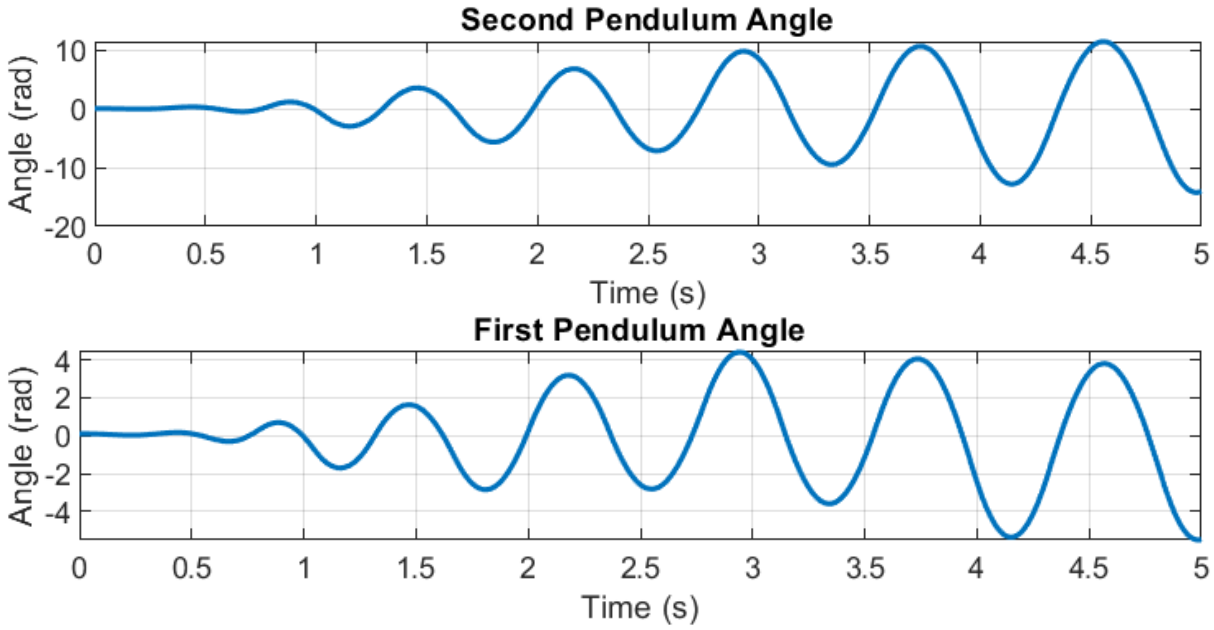

Figure 5.4 Pendulum Angle vs. Time

Observed Response:

- Initial Small Oscillations (0–2 s):
  Both pendulums begin with small oscillations, reflecting effective damping and stabilization by the controller.
- Large Oscillation Phase (2.5–4.5 s):
  As the cart deviates dramatically, both pendulum angles exhibit larger oscillations. The oscillations reach amplitudes of approximately ±0.2 rad for the first pendulum and slightly higher for the second, demonstrating the increased challenge in stabilizing the system during large transients.
- Damping and Recovery (4.5–5 s):
  In the recovery phase, the oscillations start to dampen, indicating that the controller is regaining influence over the system dynamics.

The pendulum responses validate the controller's ability to keep the pendulums from toppling, even when the cart experiences significant errors. Although the angles oscillate more during the large deviation phase, they remain within a bounded range, confirming that the stabilization strategy is effective.

5.5 Control Input Analysis

The control input (force applied to the cart) is a key indicator of the controller's aggressiveness and energy consumption. The graph below depicts the control input over time.

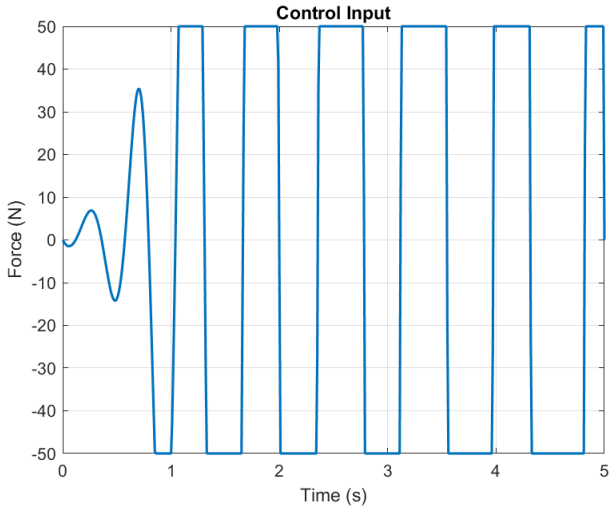

Figure 5.5 Control Input

Observed Response:

- Low Initial Effort (0–2 s):
  At the start, the control effort is minimal (within ±10 N), as the system is near equilibrium.
- Saturation Period (2–3.5 s):
  As the system dynamics become more aggressive, the control input saturates at –50 N for about 1.5 s. This is the period when the controller is applying its maximum effort to stabilize the system, particularly to prevent the pendulums from falling.
- Reversal and Recovery (3.5–4.5 s):
  The control input then abruptly reverses to +50 N, attempting to recover the cart position towards the reference.
- Final Phase (4.5–5 s):
  The input remains at or near saturation, indicating persistent high demand on the actuator.

5.6 Observer Performance

Accurate state estimation is critical for feedback control. The Luenberger observer was designed to reconstruct the full state vector from measured outputs. The performance of the observer is assessed by comparing the estimation error for key states.

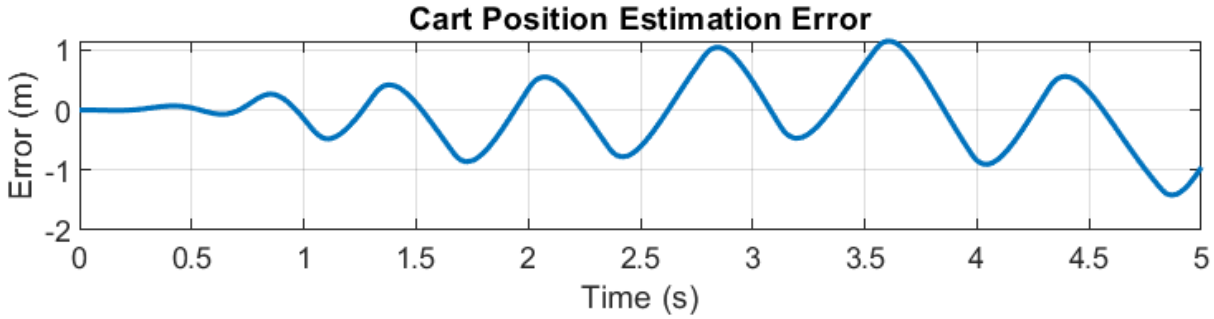

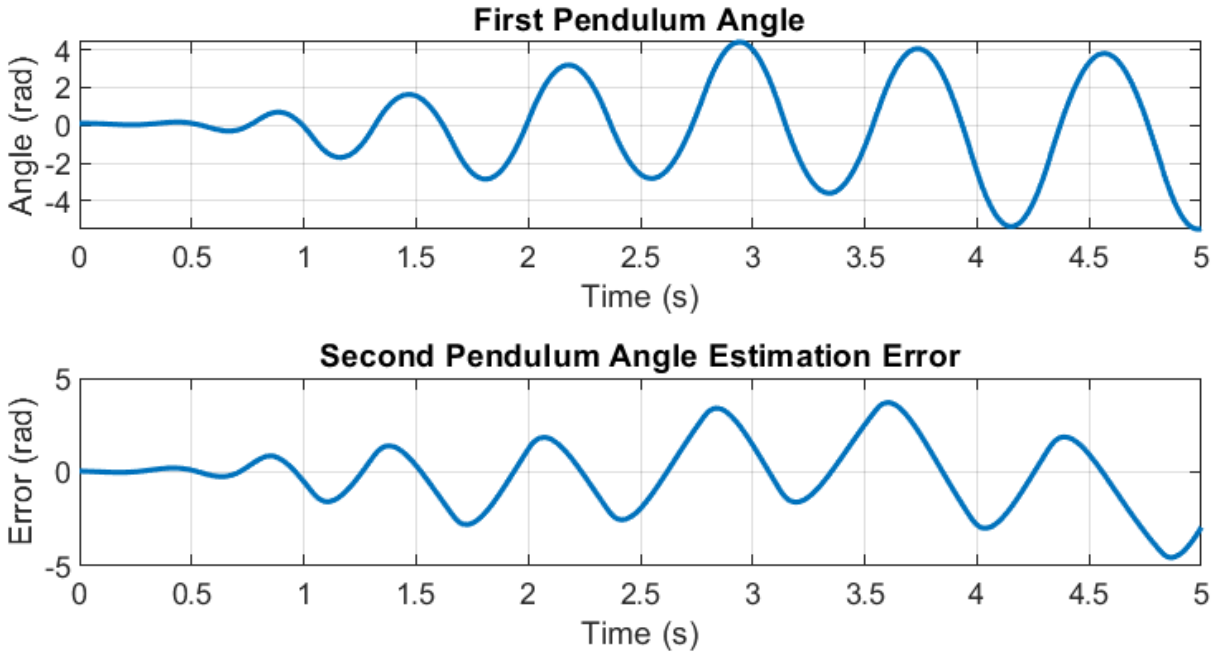

Figure 5.6 Error Estimation

Estimation Error Analysis

- **Cart Position Estimation Error:** The *First Image* shows the difference between the true cart position and its estimate. Initially, the error is negligible but increases during the large transient phase (2.5–3.5 s) to about ±2 m before recovering.
- **First Pendulum Angle Estimation Error:** As seen in *the Second Image*, the estimation error for the first pendulum angle peaks at around ±2 rad during the volatile phase, then gradually diminishes.
- **Second Pendulum Angle Estimation Error:** The *Third Image* indicates that the second pendulum's angle estimation error is even larger (up to ±5 rad) during peak dynamics but also recovers as the system stabilizes.

The observer's performance is acceptable given the large transient disturbances. The rapid convergence of the estimation error after the peak disturbances validates the choice of observer poles and gain matrix K_e. The design ensures that once the system dynamics calm down, the observer quickly aligns with the true state, enabling effective state feedback.

6. Observer and Filter Performance Comparison

This section compares two state estimation approaches: the deterministic Luenberger observer and the stochastic discrete Kalman filter. Both methods were implemented to provide state estimates for feedback control, and their performance is compared to understand their respective advantages and limitations.

6.1 Luenberger Observer Performance

The Luenberger observer employs a fixed-gain approach using a precomputed gain matrix K_e . Its design is based on placing the observer poles faster than the closed-loop controller poles to ensure rapid error convergence. The computed gain matrix is:

$$K_e = \begin{bmatrix} 0.0879 & 0.0012 & -0.0024 \\ 0.1877 & 0.0176 & -0.0077 \\ -0.0011 & 0.0839 & -0.0016 \\ -0.0133 & -0.1185 & -0.0120 \\ -0.0062 & -0.0019 & 0.0843 \\ -0.0407 & -0.0491 & -0.2143 \end{bmatrix}$$

As observed in *Figure 5.6*, the Luenberger observer achieves rapid convergence of the estimation errors following significant transients, although during high dynamic periods, the errors become non-negligible. The simplicity of the design makes it attractive when the measurement noise is low and system dynamics are well modelled.

6.2 Kalman Filter Performance

The discrete Kalman filter, on the other hand, is implemented to optimally account for both process noise and measurement noise. Its performance is governed by the noise covariances:

$$Q_{kf} = \text{diag}(0.01,\ 0.1,\ 0.01,\ 0.1,\ 0.01,\ 0.1),$$

$$R_{kf} = \text{diag}(0.01,\ 0.01,\ 0.01)$$

The Kalman filter uses a recursive prediction-update algorithm to adjust its gain at every time step, thereby minimizing the mean square error of the state estimates.

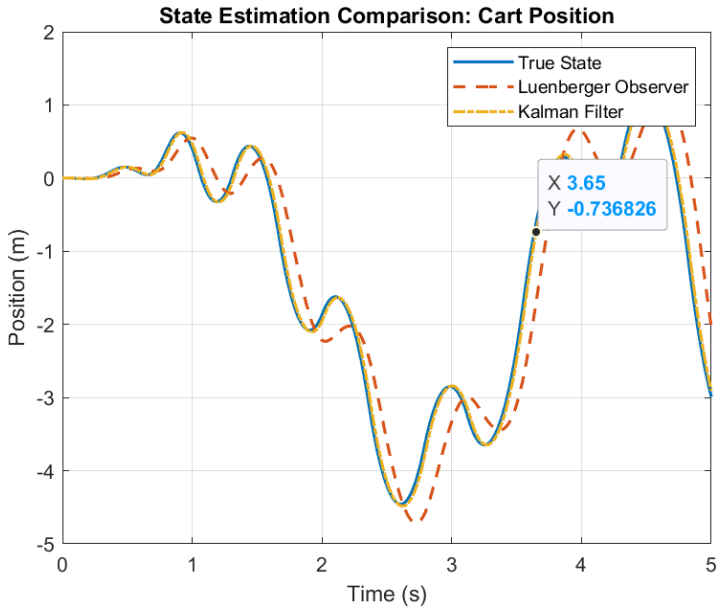

Figure 6.2 Luenberger observer vs. Kalman Filter

Figure 6.2 presents a comparison of the cart position estimates:

- The true cart position is shown as a blue solid line.
- The Luenberger observer estimate is depicted with a red dashed line.
- The Kalman filter estimate appears as a yellow dash-dotted line.

The Kalman filter's estimates are smoother during rapid transients, especially when measurement noise is present, due to its adaptive gain adjustment based on error covariance. This results in improved noise rejection compared to the fixed-gain Luenberger observer.

6.3 Discussion of Comparison

6.3.1 Convergence and Noise Rejection

- **Convergence:** Both estimation methods eventually converge to the true state. However, the Kalman filter often demonstrates a slightly slower yet smoother convergence profile compared to the Luenberger observer.
- **Noise Rejection:** The Kalman filter outperforms the Luenberger observer when dealing with significant measurement noise. Its adaptive nature allows it to dynamically adjust the weight given to the measurements versus the model predictions.

6.3.2 Complexity and Tuning

- **Luenberger Observer:** With fixed gains, the Luenberger observer is simpler to design and implement. However, it lacks adaptability in the presence of noise or unforeseen disturbances.
- **Kalman Filter:** Although the Kalman filter requires careful tuning of the covariance matrices Q_{kf} and R_{kf}, it provides an optimal estimate in the presence of noise. This adaptability can lead to more robust performance in practical applications where sensor noise and modelling errors are inevitable.

6.3.3 Overall Implications

The choice between these two estimation techniques depends on the specific requirements of the control application. For scenarios with low noise and well-characterized dynamics, a Luenberger observer may be sufficient. In contrast, in environments with higher noise levels or greater uncertainty, the Kalman filter's ability to adaptively tune its gain provides a distinct advantage.

Figure References:

- *Figure 6.2* illustrates the direct comparison of the state estimates (cart position) between the two methods.
- Additional observer performance plots (*Figure 5.6)* support this analysis by showing estimation error trends.

7. Conclusions

The digital control study for the double inverted pendulum has provided significant insights into the challenges of controlling unstable, underactuated systems. Some conclusions are as follows:

1. **Dynamic Complexity:** The eigenvalue analysis revealed unstable modes, particularly in the pendulum dynamics, which require aggressive control action. The continuous and discrete eigenvalue analyses emphasize the intrinsic instability and non-minimum phase dynamics of the system.
2. **Controller Performance:** The LQR controller with integral action successfully stabilizes the system, as demonstrated by the damping of the pendulum oscillations. However, the severe overshoot and large steady-state error in the cart position highlight the trade-offs that exists in balancing pendulum stabilization with position tracking.

3. **Input Saturation and Control Energy:** The prolonged saturation of the control input and the very high control energy reflect the high actuator demands in this control problem. These issues are intrinsic to the system's underactuated and non-minimum phase characteristics.
4. **Observer Effectiveness:** Both the Luenberger observer and the Kalman filter provided effective state estimates. The Kalman filter offered smoother performance under noise conditions, while the Luenberger observer, despite its simplicity, performed adequately in nominal scenarios.
5. **Robustness:** The robustness analysis, where the mass of the second pendulum was increased by 50%, demonstrated that the controller and observer designs are resilient to significant parameter variations, maintaining stability albeit with altered transient responses.